Filtering states with total spin on a quantum computer

Pooja Siwach [*]

Department of Physics, Indian Institute of Technology Roorkee, Roorkee-247667, Uttarakhand, India
and Department of Physics, University of Wisconsin-Madison, Madison, Wisconsin 53706, USA

Denis Lacroix [†]

Université Paris-Saclay, CNRS/IN2P3, IJCLab, 91405 Orsay, France

Starting from a general wave-function described on a set of spins or qubits, we propose several quantum algorithms to extract the components of this state on eigenstates of total spin $\mathbf{S}^2$ and its z component S_z. The method plays the role of total spin projection and gives access to the amplitudes of the initial state on a total spin basis. The different algorithms have various degrees of sophistication depending on the requested tasks. They can either solely project onto the subspace with good total spin or completely uplift the degeneracy in this subspace. In the former case, when the projection on the total spin j is made, we show that the number of operations for the projection can be reduced from a quadratic to a linear dependence in j. After each measurement, the state collapses to one of the spin eigenstates that could be used for postprocessing. For this reason, we call the method total quantum spin filtering.

I. INTRODUCTION

Quantum many-body systems interacting strongly can spontaneously break symmetries [1,2]. To quote some physical examples presenting spontaneous symmetry breaking, we mention the Cooper pairing in superfluid systems, which can be treated by breaking the U(1) symmetry associated with the particle number conservation [3–6]. Another historical example is the case of spin chains where different spontaneous spin orientations can take place [7]. In some cases, like in atomic nuclei, several symmetries can be broken simultaneously, like parity, U(1) symmetry (particle number conservation), rotational symmetry, and so on to unveil the richness of such mesoscopic systems [8–10].

A practical way to incorporate such symmetry breaking (SB) in the mean-field or Hartree-Fock (HF) approaches is to utilize the many-body trial wave-functions in the variational method, that do not respect all symmetries of the problem under interest. Such SB states are very powerful tools to grasp the complex internal correlations without requiring to go beyond the mean-field approximations.

Although the SB wave-function in variational methods can be used to treat the complex internal correlations, a precise description of physical systems requires the restoration of broken symmetries [1]. The first reason is that the experimental observations generally reflect the properties of quantum states respecting symmetries of the Hamiltonian, while the SB states correspond to a mixing of different "true" channels. Second, symmetry restoration (SR) is a practical way to include quantum fluctuations beyond the mean-field [1,2]. Such quantum fluctuations can be seen as a mixing of different SB states.

In practice, with conventional (i.e., classical) computers, SR can be performed using the projection techniques [1,8–10]. The projected wave function can then be used directly to compute the energy or more generally spectroscopic properties, leading to the so-called projection-after-variation (PAV) technique [9,10]. In a more challenging way, the SR wave function itself can be used as a trial state for the further reduction in steps of the variational method leading to the variation-after-projection (VAP) technique. The VAP technique is at the forefront of what can be done today and becomes especially complicated to perform when several symmetries are broken [10] initially.

The SB-SR is a ubiquitous technique for the description of many-body systems. Part of its success comes from the fact that SR wave-function generally corresponds to strongly entangled many-body states that properly incorporate the symmetry properties of quantum systems. Given the success of the SB-SR technique on classical computers, it is interesting to explore the possibility to construct these states on quantum computers with the aim to use them in quantum variational techniques [11–17].

Besides the applications to the physical systems mentioned above, the possibility to prepare entangled states respecting specific symmetries might have wider applications in quantum computing. Indeed, the wave functions prepared by some widely used quantum algorithms, like the hardware efficient ansatz (HEA) [18], qubit coupled cluster [19], (QEB-ADAPT)-VQE [20] to quote some of them, are not necessarily eigenstates of the particle number or total spin. The projection method presented here can be used in combination with these techniques.

The direct construction of such states using quantum circuits has already been explored for some symmetries like U(1) symmetry associated with particle number conservation [21,22]. The problem of constructing eigenstates of the total

---

[*]psiwach@physics.wisc.edu
[†]denis.lacroix@ijclab.in2p3.fr

spin directly was also considered. For example, an efficient quantum algorithm based on the Schur transformation was proposed in Ref. [23] (see also Refs. [24–27]). The construction of eigenstates of the total spin on a quantum computer has attracted a lot of attention primarily due to its usefulness in quantum many-body problems appearing in physics and chemistry [15]. Significant efforts are being made currently to prepare many-body states on quantum computers that automatically preserve the spin symmetry [22,28–31], intending to obtain more optimal states that can be used in variational calculations.

As an alternative to the direct method, we explore here the possibility to use SB followed by SR in two steps for the problem of projection onto the total spin. Some discussions related to the formulation of the SR on quantum computers using projection techniques can be found in Refs. [21,32–36]. Our work is a continuation of Ref. [36], where a method based on the measurement of ancillary qubits is used to project the wave-function and restore the symmetry. In Ref. [36], an application is explored for the restoration of the number of particles, where only a single projection is necessary.

Some advantage of the quantum algorithm compared with its equivalent on classical computers is that (i) it can *a priori* be applied to a very large Hilbert space, provided that a large number of qubits can be manipulated; (ii) it avoids the calculation of integrals [8,9] that might be tedious, especially when multiple projections are performed simultaneously. At variance, in the quantum algorithm, a projection of the system is made after each measurement, and (iii) the same circuit gives parallel access to the projections on different sub-Hilbert spaces associated with different particle numbers. We discuss here how the method can be adapted to a more complex problem such as the spin projection. One evident motivation of the present work is the development of the projection algorithm that can be used as a preprocessing prior to the use of variational methods. Second, the projection on spins is also an important intermediate step for treating more complex systems, like atomic nuclei, with spin-orbit coupling.

The algorithms we present below play the role of SR and can be seen as a filter for the symmetry-restored components. For this reason, we call it the *total quantum spin filtering* (TQSf) technique.

II. QUANTUM ALGORITHMS FOR THE PROJECTION ON TOTAL SPIN

Our starting point is an ensemble of n particles labeled by i with two components, spin up $(+)$ and spin down $(-)$. The spin components of the particles are encoded on a set of qubits $\{|s_i\rangle\}_{i=0,n-1}$ (with $s_i \in \{0, 1\}$) with the convention $|0_i\rangle = |+\rangle_i$ and $|1_i\rangle = |-\rangle_i$. The basis formed by the states $\{\bigotimes_{i=0,n-1} |s_i\rangle\}$ is called *natural basis* (NB) below. The total spin operator of the system is defined as $\mathbf{S} = \sum_i \mathbf{S}_i$, where $\mathbf{S}_i$ denotes the spin operator associated with the particle i that is linked to the standard Pauli matrices through $\mathbf{S}_i = \frac{1}{2}(X_i, Y_i, Z_i)$. These three operators are completed by the identity operator I_i.

The eigenstates of the commuting variables $\mathbf{S}^2$ and S_z also form a complete basis for the Hilbert space of n qubits. We call this basis below the *total spin basis* (TSB). The possible eigenvalues of $\mathbf{S}^2$ and S_z are given by $S(S + 1)$ and M

(assuming $\hbar = 1$), respectively, with the constraints $S \leqslant n/2$ and $-S \leqslant M \leqslant +S$. The TSB is widely used in physics and chemistry. Its properties can be found in textbooks [37–39].

In the natural basis, the system is described by the wave function

$$|\Psi\rangle = \sum_{s_i \in \{0,1\}} \Psi_{s_1,\dots,s_N} |s_1, \dots, s_n\rangle. \quad (1)$$

We consider here a system described by a Hamiltonian that commutes with both $\mathbf{S}^2$ and S_z. Therefore, the eigenstates of the Hamiltonian are also eigenstates of the total spin components. The goal of the present work is to discuss quantum algorithms that project this state on eigenstates of the total spin.

Let us introduce the set of projectors $\mathcal{P}_{[S,M]}$ that projects on the subspace associated with the eigenvalues (S, M). Our first objective is to obtain the amplitudes of the initial state decomposition $A_{S,M} \equiv \langle\Psi|\mathcal{P}_{[S,M]}|\Psi\rangle$ and eventually obtain one of the projected normalized states given by

$$|\Psi_{S,M}\rangle = A_{S,M}^{-1/2}\mathcal{P}_{[S,M]}|\Psi\rangle.$$

To achieve this objective, we apply the technique proposed in Ref. [36]. We consider two separate operators U_S and U_z, allowing for the discrimination of $\mathbf{S}^2$ and S_z eigenvalues when used in the quantum phase estimation (QPE) algorithm [40–43]. As a result, the projection on the states $|\Psi_{S,M}\rangle$ is automatic when the ancillary qubits used in the QPE are measured.

The operators used to discriminate the different components are taken as $U_{S/z} = e^{2\pi i \alpha_{S/z}(n) O_{S/z}}$, where O_S and O_z are operators with known eigenvalues. The eigenvalues, denoted by $\{\lambda_i^S\}$ and $\{\lambda_i^z\}$, are proportional to those of $\mathbf{S}^2$ and S_z, respectively. Furthermore, $\alpha_S(n)$ and $\alpha_z(n)$ should be chosen in a very specific way. These parameters should ensure that, for all eigenvalues, the quantities $\alpha_x(n)\lambda_i^x$ verifies $0 \leqslant \alpha_x(n)\lambda_i^x < 1$ and that these quantities always correspond to a binary fraction with a finite number of terms. Moreover, denoting the number of extra ancillary qubits used in the QPE by n_S and n_z, respectively, for U_S and U_z, these numbers should be chosen as the minimal values such that $2^{n_x}\alpha_x(n)\lambda_i^x$ are positive integers for all eigenvalues.

There is some flexibility in the choice of both U_S and U_z. First, we consider the total S_z component. This component verifies

$$S_z = N_0 - N_1 \text{ with } N_0 + N_1 = nI,$$

where $N_0 = \frac{1}{2}\sum_k(I_k + Z_k)$ $[N_1 = \frac{1}{2}\sum_k(I_k - Z_k)]$ is the operator that counts the number of 0 (the number of 1 in the state). S_z, N_0, and N_1 are commuting operators, and the states of the natural basis are eigenstates of these operators. To select the states with good particle number or, equivalently, eigenstates of S_z, we use the QPE applied on N_1. With the constraint listed above, a convenient choice is

$$U_z = \exp\left\{2\pi i \frac{N_1}{2^{n_z}}\right\}. \quad (2)$$

The eigenvalues of N_1 range from zero to n. Accordingly, the minimal possible value for n_z is such that $n_z > \ln n / \ln 2$. With this choice, the filtering of states with respect to the eigenvalues of S_z becomes strictly equivalent to the particle
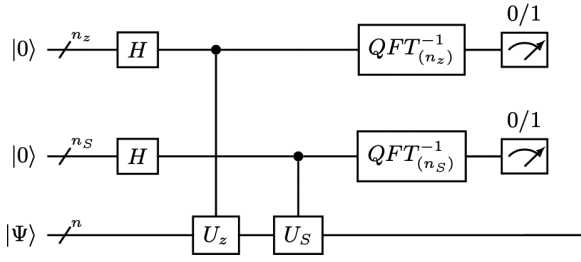
FIG. 1. Schematic illustration of the circuit used in the present work to project the states onto eigenstates of the total spin $\mathbf{S}^2$ and S_z

number projection illustrated in Ref. [36]. Therefore, in the natural basis, U_z is given by a product of phase operators

$$U_z = \prod_k \begin{bmatrix} 1 & 0 \\ 0 & e^{i\pi/2^{n_z-1}} \end{bmatrix}_k .$$

We now consider the projection on total spin $\mathbf{S}^2$. For n qubits, the eigenvalues of this operator are positive and verify $\lambda_S \leqslant n(n+2)/4$. Depending on the fact that n is even or odd, we propose the following forms of U_S^e and U_S^o:

$$U_S^e = \exp\left\{2\pi i \frac{\mathbf{S}^2}{2^{n_S+1}}\right\}, \quad U_S^o = \exp\left\{2\pi i \frac{(\mathbf{S}^2 - 3/4)}{2^{n_S}}\right\}. \quad (3)$$

The number of ancillary qubits has the constraints

$$n_S > \frac{\ln k(k+1)}{\ln 2} - 1 \text{ (even)}, \quad n_S > \frac{\ln k(k+2)}{\ln 2} \text{ (odd)}, \quad (4)$$

respectively, for even $n = 2k$ and odd $n = 2k + 1$ cases.

In practice, to compute the operators U_S^e and U_S^o, we use the standard formula [44]

$$\mathbf{S}^2 = \frac{n(4-n)}{4} I + \sum_{i<i',i'=0}^{n-1} P_{ii'}, \quad (5)$$

which generalizes the Dirac identity originally derived for two spins in Ref. [45]. The set of operators $P_{ii'}$ are the transposition

operators given by

$$P_{ii'} = \frac{1}{2}(I + X_i X_{i'} + Y_i Y_{i'} + Z_i Z_{i'}).$$

We have in particular $P_{ii'}|\delta_i \delta_{i'}\rangle = |\delta_{i'} \delta_i\rangle$ and $P_{ii'}^2 = I$. With the formula given in Eq. (5), the well-known link between total spin operator and the permutation group becomes explicit [39]. Some aspects of transpositions and their use in directly constructing states with good total spins were discussed in Ref. [31]. In the quantum computing context, the transposition operators are nothing but the SWAP operators. In the present work, we implement the U_S operators [Eq. (3)] by using the Trotter-Suzuki decomposition technique [15,46] based on the expression given by Eq. (5) and by noting that

$$e^{i\alpha P_{ii'}} = \cos(\alpha)I + iP_{ii'} \sin(\alpha). \quad (6)$$

A schematic diagram of the circuit to perform the simultaneous selection of eigenstates of S_z and $\mathbf{S}^2$ is shown in Fig. 1.

The method proposed here is tested by using the IBM toolkit qiskit [47]. We show in Fig. 2 the amplitudes obtained for a system described on $n = 4$ qubits by measuring the ancillary qubits of the circuit shown in Fig. 1 for two examples of initial states. For such a small number of qubits, the decomposition in terms of the $|\Psi_{S,M}\rangle$ can be obtained analytically. We have checked that the amplitudes obtained with the measurement are consistent with the analytical ones within the errors due to the finite number of measurements.

We can further analyze the results obtained. Results displayed in Fig. 2(a) correspond to an initial state that is completely symmetric with respect to any permutation of the qubit indices. Consequently, it only decomposes on state $|\Psi_{S,M}\rangle$ that also has this property. Such states correspond to the states with the maximal possible eigenvalue of $\mathbf{S}^2$, i.e., in our case, $S = 2$. In the context of group theory, the irreducible representation associated with the TSB can be represented by the Young tableau [37–39] with a maximum of two rows. Fully symmetric states are those represented with a single row. For a general initial state with n qubits given by $|\Psi\rangle = \prod_{k=0}^{n-1} H_k |0\rangle$, its decomposition onto the TSB will be given by

$$|\Psi\rangle = \sum_{k=0}^{n} \sqrt{p_k} |\Psi_{S=n/2, S_z=n/2-k}\rangle, \quad (7)$$
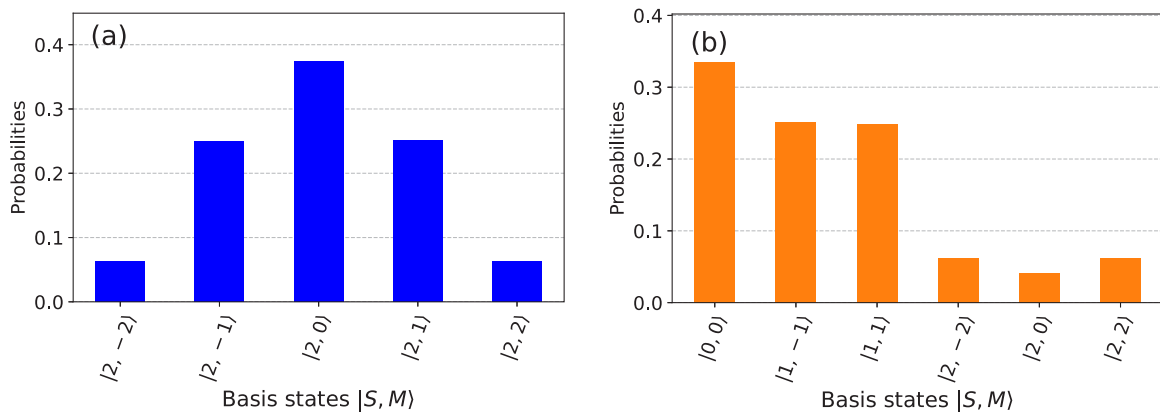
FIG. 2. Illustration of the results obtained for a system described on $n = 4$ qubits. In this case, the optimal choice for the number of ancillary qubits are $n_S = 2$ and $n_z = 3$. Results are obtained for an initial state $|\Psi\rangle = \prod_{k=0}^{3} H_k |0\rangle$ [panel (a)] and $|\Psi\rangle = X_1 X_3 \prod_{k=0}^{3} H_k |0\rangle$ [panel (b)] using the qiskit software with 10^5 shots of the qasm simulator. Here H_k denotes the Hadamard gate.

where k is the eigenvalue associated with N_1. For this specific initial state, the amplitudes p_k are equal to $C_n^k/2^n$ identifying with a binomial distribution (with $p = q = 1/2$). In the large-n limit, this probability will tend to a Gaussian probability.

We now come to the main goal of the present algorithm. When measurements are performed on the two sets of ancillary qubits respectively associated with U_S and U_z, after each measurement labeled by (λ), the total wave function $|\Psi_f^{(\lambda)}\rangle$ identifies with

$$\left|\Psi_f^{(\lambda)}\right\rangle = |S^{(\lambda)}\rangle \otimes |M^{(\lambda)}\rangle \otimes |\Psi_{S^{(\lambda)},M^{(\lambda)}}\rangle. \tag{8}$$

Here, $S^{(\lambda)}$ ($M^{(\lambda)}$) should be interpreted as the binary number obtained by measuring the ancillary qubits associated with U_S (U_z) in the event λ. So, after the measurement, the wave function $|\Psi_f^{(\lambda)}\rangle$ is an eigenstate of both the total spin and its azimuthal component. Said differently, the circuit represented in Fig. 1 plays the role of a funnel that lets only one component (S, M) pass at each event. The circuit therefore acts as as a projector that restores the total spin symmetry.

The values $(S^{(\lambda)}, M^{(\lambda)})$ might change at each measurement unless the initial state is already an eigenstate of the total spin operators. In general, the outcome of the circuit can be controlled solely through the control of the initial state (1). Consecutively, the projected state can be used for postprocessing. A direct application of the present method in physics or chemistry is to study spin systems that encounter spontaneous symmetry breaking associated with a preferred spin orientation. If we assume that the initial state depends on a set of parameters $\{\theta_i\}_{i=1,g}$, the symmetry-restored state can then be used in variational approaches both prior (projection after variation) or after the projection (projection before variation) (see, for instance, Refs. [1,8]).

The circuit of Fig. 1 helps in achieving our first objective, which is the preparation of states with good total spin and total z projection. This technique also works if the initial state is not fully symmetric with respect to the permutation of qubits. An example of such application is given in Fig. 2(b). As we see, in this case, the states will also have components of total spin with $S < n/2$, i.e., the states corresponding to a Young tableau with two rows. There is, however, a difference between the fully symmetric (FS) case and the other cases. In the FS case, the Hilbert space associated with the eigenvalues (S, M), denoted by $\mathcal{H}_{S,M}$, contains only one eigenvector of $\mathbf{S}^2$ and S_z. In other cases, i.e., for $\mathcal{H}_{S,M}$ with $S < n/2$, the Hilbert space contains an ensemble of degenerate eigenstates. For instance, in the $n = 4$ qubit case, the space $\mathcal{H}_{0,0}$ contains two states, while $\mathcal{H}_{1,M}$ with $M = -1, 0, 1$ contains three states. We denote by $d_{(S,M)}$ the size (degeneracy) of the $\mathcal{H}_{S,M}$ Hilbert space. In the degenerate case, the system state in Eq. (8) obtained after measuring the ancillary qubits will be an admixture of the different eigenstates, where the mixing coefficients will directly reflect the relative proportion of the degenerate states in the initial wave function.

III. CALCULATION OF INITIAL STATE DECOMPOSITION ON THE COMPLETE TOTAL SPIN BASIS

Let us now consider a complete basis formed by eigenstates of $\mathbf{S}^2$ and S_z. We denote one element of the basis by $|S, M\rangle_g$. The indices $g = 1, d_{S,M}$ are introduced to dissociate different states belonging to the space $\mathcal{H}_{S,M}$. The system's initial state $|\Psi\rangle$ can be decomposed as

$$|\Psi\rangle = \sum_{S,M} \sum_{g=1}^{d_{S,M}} c_{S,M}^g |S, M\rangle_g. \tag{9}$$

When $d_{S,M} = 1$, the state $|S, M\rangle_1$ will be identical with the state $|\Psi_{S,M}\rangle$ introduced previously. Otherwise, $|\Psi_{S,M}\rangle$ is an admixture of the states $|S, M\rangle_g$. Here, we intend to generalize the circuit proposed in Fig. 1 in order to obtain the amplitudes $|c_{S,M}^g|^2$ and to obtain directly the amplitude of the initial-state basis on the complete TSB formed by the states $|S, M\rangle_g$.

Coming back to the Young tableaux representation, all states that are not fully symmetric have two rows. Let us assume that these states correspond to l_1 and l_2 blocks on the first and second row, respectively (with $l_2 \leqslant l_1$ and $l_1 + l_2 = n$). The associated total spin corresponds to $S = (l_1 - l_2)/2$. The different $|S, M\rangle_g$ have the same (l_1, l_2) but differ in their symmetries with respect to the exchange of qubits. Each state can be associated with a different sequence of Young tableaux when including each spin or qubit one after the other [37,48,49] (see, for instance, Fig. 4 of Ref. [49]). The sequence of the Young tableau can be seen as an iterative procedure, where the total spin of n qubits is obtained by coupling one spin at a time. Starting from one spin, a second spin is added and an eigenstate of the operator $\mathbf{S}_{[2]}^2$ is obtained. Here, the subscript "[2]" indicates that the operator refers only to the first two spins. Consecutively, a third spin is coupled to find an eigenvector of $\mathbf{S}_{[3]}^2$, and so on, until the eigenstate of $\mathbf{S}_{[n]}^2$ is obtained [48,49]. For a system with n qubits exactly, $\mathbf{S}_{[n]}^2$ identifies with the total spin $\mathbf{S}^2$ defined previously. In the following, we denote the total spin eigenvalue for the first k qubits by $S_{[k]}$ such that the eigenvalue of $\mathbf{S}_{[k]}^2$ is equal to $S_{[k]}(S_{[k]} + 1)$.

As an illustration, we consider the $n = 4$ case used in Fig. 2. The states $|1, M\rangle$ can be generated by the three sequences of Young tableau given by

$$\tag{10}$$

Omitting $S_{[1]}$ that is always equal to $1/2$, the three sequences in Eq. (10) correspond to the set of eigenvalues for $[S_{[2]} \rightarrow S_{[3]} \rightarrow S_{[4]}]$ respectively given by (a) $[1 \rightarrow 3/2 \rightarrow 1]$, (b) $[1 \rightarrow 1/2 \rightarrow 1]$, and (c) $[0 \rightarrow 1/2 \rightarrow 1]$.

There are several important properties to be recalled here. First, there is a one-to-one correspondence between the Young tableaux sequence and a state of the irreducible representation. Second, the state constructed by a Young tableaux sequence
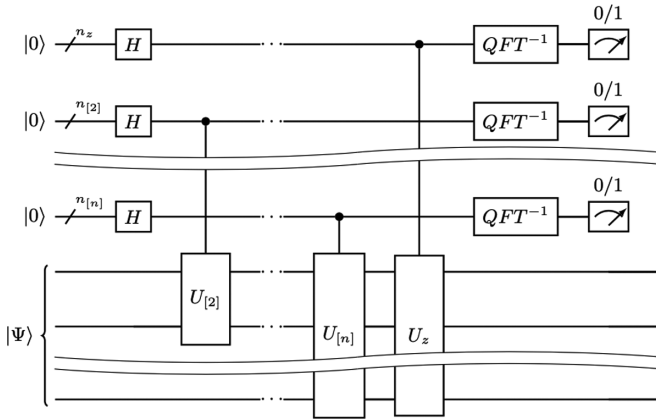
FIG. 3. Illustration of the circuit used to obtain the amplitudes $|c_{S,M}^g|^2$. After each measurement, the final state of the system collapses to one of the states of the irreducible representation $|S, M\rangle_g$.

has a "memory" of its path, i.e., it is an eigenvalue of the full set of operators $\mathbf{S}_{[2]}^2, \ldots, \mathbf{S}_{[n]}^2$ along with the total S_z components. This last property gives us a direct way to generalize the circuit given in Fig. 1 and obtain the amplitudes in Eq. (9). A brute-force technique consists of introducing a set of ancillary qubits and perform independent QPEs for all the operators $\mathbf{S}_{[j]}^2$ together with the QPE associated with the total S_z component. In practice, the QPE on a specific total spin $\mathbf{S}_{[j]}^2$ is associated to a unitary operator denoted by $U_{[j]}$, which can be constructed in a similar way as the operators defined in Eq. (3) depending on whether j is odd or even. The operators $U_{[j]}$ are deduced simply by replacing $\mathbf{S}^2$ with $\mathbf{S}_{[j]}^2$ and by optimizing the number of ancillary qubits $n_{[j]}$ according to the accessible eigenvalues of $\mathbf{S}_{[j]}^2$ as prescribed in Eq. (4).

The corresponding circuit is shown in Fig. 3. This circuit is implemented to perform calculations utilizing qiskit [47], and the results obtained for the same condition as in Fig. 2(b) are shown in Fig. 4. We see in this figure that the amplitudes
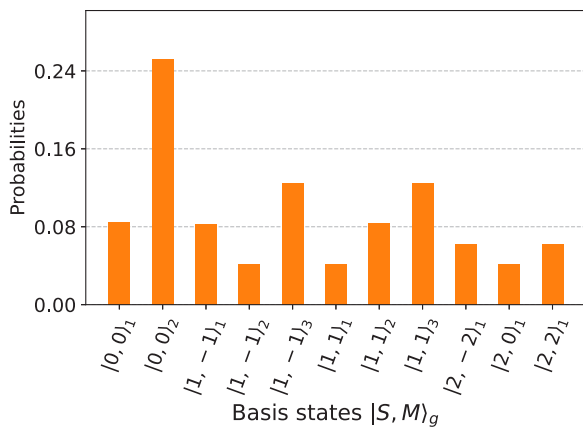
FIG. 4. Results obtained for a system described on $n = 4$ qubits with the same initial state as in Fig. 2(b) but using the circuit shown in Fig. 3. The degeneracy in the components of states $|1, -1\rangle$, $|1, 1\rangle$, and $|0, 0\rangle$ is uplifted, leading to three, three, and two separated components, respectively. The probabilities along vertical axis are the amplitudes $|c_{S,M}^g|^2$.

associated previously with the two components $|\Psi_{1,M}\rangle$ with $M = -1, 1$ have now systematically split into three amplitudes corresponding to the three states $|1, M\rangle_{g=1,2,3}$. Similarly, the component associated with $|\Psi_{0,0}\rangle$ is now separated into the two contributions $|0, 0\rangle_0$ and $|0, 0\rangle_1$. Here, again, the algorithm has been validated by confronting the amplitudes obtained numerically with the analytical ones. Finally, we mention that the outcome of the circuit after each measurement is one of the states of the irreducible total spin representation.

A. Reducing the circuit depth of the total quantum spin filtering method

The brute-force generalization of the algorithm to project a given state onto one of the irreducible representations of the total spin requires a rather larger number of operations and of ancillary qubits. As seen in Eq. (5), the number of transpositions in $\mathbf{S}_{[j]}^2$ is equal to $j(j-1)/2$. Therefore, if the Trotter-Suzuki technique is employed to simulate the operator $U_{[j]}$, the exponential appearing in this operator have *a priori* also to be split into $j(j-1)/2$ terms showing that the decomposition scales quadratically with j. To reduce the numerical efforts, we first note that the states $|S, M\rangle_g$ are also eigenstates of the difference $\mathbf{S}_{[j]}^2 - \mathbf{S}_{[j-1]}^2$ for $2 \geqslant j \geqslant n$. Since we have

$$\mathbf{S}_{[j]}^2 - \mathbf{S}_{[j-1]}^2 = \frac{5 - 2j}{4} + \sum_{i<j} P_{ij}, \qquad (11)$$

we finally remark that these states are the eigenstates of the set of simpler operators given by

$$H_{[j]} = \sum_{i<j} P_{ij}, \qquad (12)$$

for $j = 2, \ldots, n$. The eigenvalues of a given operator $H_{[j]}$ are integers and lie in the interval $[-1, j-1]$. The set of eigenvalues of the $H_{[j]}$ also uniquely defines a state of the irreducible representation. If we denote an eigenvalue of $H_{[j]}$ by $h_{[j]}$, the three different paths displayed in Eq. (10) correspond to the sequences $[h_{[2]} \to h_{[3]} \to h_{[4]}]$ respectively given by (a) $[+1 \to +2 \to -1]$, (b) $[+1 \to -1 \to +2]$, and (c) $[-1 \to +1 \to +2]$. Therefore, they can be used as an alternative of the $\mathbf{S}_{[j]}^2$ in the previous algorithm. A proper choice of the $U_{[n]}$ is then

$$U_{[n]} = \exp\left\{ 2\pi i \frac{[H_{[j]} + 1]}{2^{n_{[j]}}} \right\}, \qquad (13)$$

where $n_{[j]}$ is optimally chosen as the minimal value of $n_{[j]}$ verifying for $j \geqslant 2$

$$n_{[j]} > \frac{\ln(j-1)}{\ln 2}. \qquad (14)$$

The use of $H_{[j]}$ instead of $\mathbf{S}_{[j]}^2$ has two practical advantages. As seen from Eq. (12), these operators contain only $(j-1)$ transpositions, and therefore the number of terms in the Trotter-Suzuki method will scale linearly with j compared with the quadratic number of terms for $\mathbf{S}_{[j]}^2$. This reduction from quadratic to linear scaling is a significant improvement in the algorithm proposed here compared with the original one. In addition, the number of ancillary qubits $n_{[j]}$ obtained

from the condition given in Eq. (14) will also be much lower than the one obtained from the previous condition given in Eq. (4) when j increases. We have also implemented the TQSf approach based on the operators $\{H_{[j]}\}$ for the illustration given in Fig. 4 and have obtained strictly the same results (not shown here) but with fewer operations.

B. Total quantum spin filtering method based on sequential measurements technique with minimal quantum resources

In the previous discussion, we have explored the possibility of obtaining the amplitudes of any state on the total spin basis by performing the simultaneous measurements of a set of ancillary qubits. These measurements give a snapshot of the paths of each total spin eigenvectors in the so-called sequential construction of the state.

As underlined in Ref. [48] and further discussed recently in Refs. [27,49], one can associate a binary number to each path representing directly the increase or decrease of the total spin components or Young tableaux construction (see Fig. 4 of Ref. [49]). Thus, considering the three examples of paths in Eq. (10) again, the different paths can indeed be represented by (a) [↗↗↘], (b) [↗↘↗], and (c) [↘↗↗] that can be associated with the three binary numbers 110, 101, and 011, respectively.

A possible manner to directly encode the increase or decrease of the total spin on a single qubit is to find an appropriate operator to encode this property. Let us assume that we have $j-1$ qubits already having a total spin $S_{[j-1]}$ that is known. If we add one more spin, the new total spin that is accessible to the complete set of spins will be $S_{[j]} = S_{[j-1]} \pm 1/2$ (note that $S_{[j-1]} = 0$ imposes $S_{[j]} = S_{[j-1]} + 1/2$). A simple analysis shows that the following operator:

$$G_{[j]} = \frac{\mathbf{S}_{[j]}^2 - \mathbf{S}_{[j-1]}^2 + S_{[j-1]} + \frac{1}{4}}{(2S_{[j-1]} + 1)}, \qquad (15)$$

has an eigenstate of the total spin with an eigenvalue equal to 1 (0) for the eigenstate associated with the spin $S_{[j]} = S_{[j-1]} + 1/2$ ($S_{[j]} = S_{[j-1]} - 1/2$). Therefore, this operator directly encodes the increase or decrease of the total spin when adding the spin j.

A crucial aspect of the application of the operator $G_{[j]}$ is that (i) the mapping to a single binary digit is valid only if the set of $j-1$ spins are already projected onto eigenstates of the total spin $\mathbf{S}_{[j-1]}^2$ and (ii) the eigenvalue $S_{[j-1]}$ is known. Assuming that these two conditions are fulfilled, it is worth mentioning that a single ancillary qubit will be necessary to perform the QPE method for the $G_{[j]}$ operator. The unitary operator to be used in the QPE is given by

$$V_{[j]} = \exp\{\pi i G_{[j]}\}, \qquad (16)$$

and the QPE reduces to a simple Hadamard test.

The two conditions above suggest a modified algorithm with an iterative procedure for the measurements with a successive set of projections on the $\mathbf{S}_{[j]}^2$ with increasing j. We restart from a system $|\Psi\rangle$ described on a set of n spins. We introduce a variable S that will be updated at each measurement and equal to the $S_{[j]}$ value at step j. Initially, $S = 1/2$, i.e., the total spin for a single-spin case. Consecutively, we make the set of Hadamard tests or measurements iteratively as follows:

$S = \frac{1}{2}, j = 1$
while $j \neq n$ do
$\quad j \to j + 1$
$\quad$ if $S \neq 0$ do
$\quad\quad S_{[j]} = S$
$\quad\quad$ Perform the Hadamard test with $V_{[j]}$
$\quad\quad$ Measure the ancillary qubit
$\quad\quad M = $ result of the measurement (0 or 1)
$\quad\quad S \to S + M - \frac{1}{2}$
$\quad$ else do
$\quad\quad S \to S + \frac{1}{2}$
$\quad$ end if
end while
$S_{[n]} = S$

One difficulty in the algorithm is that the intermediate step j is triggered by the knowledge of $S_{[j-1]}$ and more generally of the total spins components $S_{[k]}$ with $k < j$. Assuming ideally that the interface from a quantum to a classical computer works perfectly, the above algorithm can be implemented by using sequentially a set of Hadamard tests for the operators $V_{[k]}$ with increasing k. Explicitly, starting from the initial state $|\Psi\rangle$, a Hadamard test is performed using $V_{[2]}$; after the ancillary qubit measurement, the value of S is updated on the classical computer and the new operator $V_{[3]}$ is constructed. Then, a second Hadamard test is made on the system using $V_{[3]}$, and so on, until all Hadamard tests are performed. This procedure is nothing but a quantum algorithm with repeated controlled operations by the classical computer.

(a)   (b)
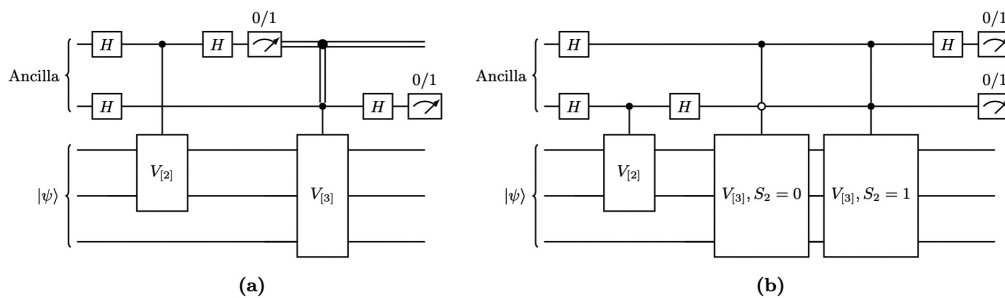
FIG. 5. Quantum circuits for a three spin system to implement the technique for Young tableaux to encode the path of total spin. (a) The circuit with the controlled operations on classical bits based on the measurement outcome from previous step. Double lines represent the classical bits. (b) An alternative circuit based on the principle of deferred measurement [40], suitable for currently available real quantum hardware. These circuits can be extended for a larger spin system in a similar manner.
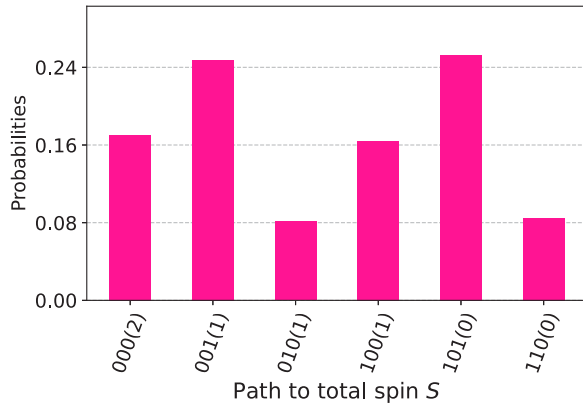
FIG. 6. Illustration of the results obtained for a system described on $n = 4$ qubits with the same initial state as in Fig. 2(b) but using the circuit shown in Fig. 5(b). The 0(1) in the bit strings on horizontal axis represents the increase (decrease) in the spin, and the total spin S is given in parentheses. The path represented by the bit strings should be read from right to left.

We show in Fig. 5 the circuit for a three-spin case to perform this scheme [Fig. 5(a)]. We start with considering two spins and, after measurement, the resulting value (0 or 1) stored in the classical bit is utilized to control the form of operator $V_{[j]}$ to be considered for the three spin case. Furthermore, by adding one more ancilla qubit for each spin, and the controlled operations using the values stored previously on classical bits, we can extend this circuit to explore the larger spin or qubit systems.

Considering the same initial state as used in Fig. 2(b), the results obtained from the extension of circuit Fig. 5(a) to the four-qubit or -spin case are given in Fig. 6. As a straightforward validation, we can see that the contribution of total S is the same as given in Fig. 4. To obtain the irreducible representation, we can project the S_z in the same way as performed in the earlier two techniques.

We finally mention that conditional operators on the classical register are currently not supported on the available real quantum devices. Therefore, we also explore the possibility to apply the present procedure without requesting classical controlled operations. An alternative procedure is to use the circuit given in Fig. 5(b), which is based on the principle of deferred measurement [40]. This procedure for the three qubit case essentially leads to the same results. But this circuit has complexities in the form of multicontrolled gates, which need to be further decomposed into single- and two-qubit gates.

IV. CONCLUSIONS

We have extended the strategy proposed in Ref. [36] to develop the quantum algorithm to project a general wave function described on a set of spins or qubits onto eigenstates of the total spin and its projection on the z axis. We call this algorithm the total quantum spin filtering (TQSf) because it acts as a filter for components having specific properties. We start with the brute-force method based originally on the QPE and requires several controlled operations that scale quadratically with the total spin value. Guided by the properties of the permutation group and more specifically on the sequence of Young tableaux to construct a symmetric state, we propose a technique in which the number of controlled operations scales linearly with the spin. Such an alternative algorithm should be more suited for applications of near-term quantum platforms. Recently, an algorithm named the "Rodeo algorithm" [50,51] was proposed that can be used as an alternative to the QPE, opening new perspectives for applications during the "noisy intermediate-scale quantum" (NISQ) period. It would be interesting to investigate how the different projection methods we propose here can be combined with or take advantage of the Rodeo method.

The primary motivation of the present work is the preparation of wave functions that uses the symmetry-breaking and symmetry-restoration method to grasp complex internal correlations in quantum many-body systems. The states obtained here, after projection, are strongly entangled and can be directly used as inputs for variational methods. This variation-after-projection method [1,8] is known to be rather effective, but states obtained in this way, especially when several symmetries are restored simultaneously, are difficult to manipulate on a classical computer. It is worth noting that the projection can *a priori* be combined with any existing methods which are popular today to prepare trial states on qubits and that do not necessarily respect the total spin or particle number projection [18,20,33]. An illustration of the combined use of variational and filtering technique was made in Refs. [52] underlying the great potential of our approach.

Finally, and although this is not the original motivation of the present problem, because of the close connection between total spin space and symmetric group, one might anticipate that the projection technique can also be used in complex combinatorial problems. As a straightforward example, one might assume that the states $|0_i\rangle$ and $|1_i\rangle$ encode the result "No" or "Yes" to a certain query by an element "i" of a set. The projection technique can then be directly used to perform data mining, such as isolating components with a given number of "Yes" and computing the associated probabilities.

[1] J. P. Blaizot and G. Ripka, *Quantum Theory of Finite Systems* (MIT Press, Cambridge, 1986).

[2] A. Atland and B. D. Simons, *Condensed Matter Field Theory* (Cambridge University Press, Cambridge, 2010).

[3] J. von Delft and D. C. Ralf, Spectroscopy of discrete energy levels in ultrasmall metallic grains, Phys. Rep. **345**, 61 (2001).

[4] V. Zelevinsky and A. Volya, Nuclear pairing: New perspectives, Phys. At. Nucl. **66**, 1781 (2003).

[5] J. Dukelsky, S. Pittel, and G. Sierra, Colloquium: Exactly solvable Richardson-Gaudin models for many-body quantum systems, Rev. Mod. Phys. **76**, 643 (2004).

[6] D. M. Brink and R. A. Broglia, *Nuclear Superfluidity: Pairing in Finite Systems* (Cambridge University Press, Cambridge, 2005).

[7] A. Auerbach, *Interacting Electrons and Quantum Magnetisms* (Springer-Verlag, New York, 1994).

[8] P. Ring and P. Schuck, *The Nuclear Many-Body Problem* (Springer-Verlag, New York, 1980).

[9] M. Bender, P.-H. Heenen, and P.-G. Reinhard, Self-consistent mean-field models for nuclear structure, Rev. Mod. Phys. **75**, 121 (2003).

[10] L. M. Robledo, T. R. Rodríguez, and R. R. Rodríguez-Guzmán, Mean field and beyond description of nuclear structure with the Gogny force: a review, J. Phys. G **46**, 013001 (2018).

[11] A. Peruzzo, J. McClean, P. Shadbolt, M.-H. Yung, X.-Q. Zhou, P. J. Love, A. Aspuru-Guzik, and J. L. O'Brien, A variational eigenvalue solver on a photonic quantum processor, Nat. Commun. **5**, 4213 (2014).

[12] J. R. McClean, J. Romero, R. Babbush, and A. Aspuru-Guzik, The theory of variational hybrid quantum-classical algorithms, New J. Phys. **18**, 023023 (2016).

[13] Y. Cao *et al.*, Quantum chemistry in the age of quantum computing, Chem. Rev. (Washington, DC, U. S.) **119**, 10856 (2019).

[14] M. Cerezo *et al.*, Variational quantum algorithms, Nat. Rev. Phys. **3**, 625 (2021).

[15] S. McArdle, S. Endo, A. Aspuru-Guzik, S. C. Benjamin, and X. Yuan, Quantum computational chemistry, Rev. Mod. Phys. **92**, 015003 (2020).

[16] S. Endo, Z. Cai, S. C. Benjamin, X. Yuan, Hybrid quantum-classical algorithms and quantum error mitigation, J. Phys. Soc. Jpn. **90**, 032001 (2021).

[17] K. Barthi *et al.*, Noisy intermediate-scale quantum (NISQ) algorithms, arXiv2101.08448.

[18] T. Keen, T. Maier, S. Johnston, and P. Lougovski, Quantum-classical simulation of two-site dynamical mean-field theory on noisy quantum hardware, Quantum Sci. Technol. **5**, 035001 (2020).

[19] I. G. Ryabinkin, T.-C. Yen, S. N. Genin, and A. F. Izmaylov, Qubit coupled cluster method: A systematic approach to quantum chemistry on a quantum computer, J. Chem. Theory Comput. **14**, 6317 (2018).

[20] Y. S. Yordanov, V. Armaos, C. H. Barnes, and D. R. Arvidsson-Shukur, Qubit-excitation-based adaptive variational quantum eigensolver, Commun. Phys. **4**, 228 (2021).

[21] N. Moll, A. Fuhrer, P. Staar, and I. Tavernelli, Optimizing qubit resources for quantum chemistry simulations in second quantization on a quantum computer, J. Phys. A: Math. Theor. **49**, 295301 (2016).

[22] B. T. Gard, L. Zhu, G. S. Barron, N. J. Mayhall, S. E. Economou, and E. Barnes, Efficient symmetry-preserving state preparation circuits for the variational quantum eigensolver algorithm, npj Quantum Inf. **6**, 10 (2020).

[23] D. Bacon, I. L. Chuang, and A. W. Harrow, Efficient Quantum Circuits for Schur and Clebsch-Gordan Transforms, Phys. Rev. Lett. **97**, 170502 (2006).

[24] W. Kirby, A practical quantum Schur transform, Undergraduate thesis, Williams College, 2017.

[25] W. M. Kirby and F. W. Strauch, A practical quantum algorithm for the Schur transform, Quantum Inf. Comput. **18**, 721 (2018).

[26] H. Krovi, An efficient high dimensional quantum Schur transform, Quantum **3**, 122 (2019).

[27] V. Havlicek and S. Strelchuk, Quantum Schur Sampling Circuits can be Strongly Simulated, Phys. Rev. Lett. **121**, 060505 (2018).

[28] K. Sugisaki, S. Yamamoto, S. Nakazawa, K. Toyota, K. Sato, D. Shiomi, and T. Takui, J. Phys. Chem. A **120**, 6459 (2016).

[29] K. Sugisaki, S. Yamamoto, S. Nakazawa, K. Toyota, K. Sato, D. Shiomi, and T. Takui, Open shell electronic state calculations on quantum computers: A quantum circuit for the preparation of configuration state functions based on Serber construction, Chem. Phys. Lett. **737**, 100002 (2019).

[30] J.-G. Liu, Y.-H. Zhang, Y. Wan, and L. Wang, Variational quantum eigensolver with fewer qubits, Phys. Rev. Res. **1**, 023025 (2019).

[31] K. Seki, T. Shirakawa, and S. Yunoki, Symmetry-adapted variational quantum eigensolver, Phys. Rev. A **101**, 052340 (2020).

[32] J. D. Whitfield, Communication: Spin-free quantum computational simulations and symmetry adapted states, J. Chem. Phys. **139**, 021105 (2013).

[33] I. G. Ryabinkin and S. N. Genin, Symmetry adaptation in quantum chemistry calculations on a quantum computer, arXiv:1812.09812 v1.

[34] T.-C. Yen, R. A. Lang, and A. F. Izmaylov, Exact and approximate symmetry projectors for the electronic structure problem on a quantum computer, J. Chem. Phys. **151**, 164111 (2019).

[35] T. Tsuchimochi and Y. Mori, Spin-projection for quantum computation: A low-depth approach to strong correlation, Phys. Rev. Res. **2**, 043142 (2020).

[36] D. Lacroix, Symmetry-Assisted Preparation of Entangled Many-Body States on a Quantum Computer, Phys. Rev. Lett. **125**, 230502 (2020).

[37] A. Messiah, *Quantum Mechanics* (North-Holland, Amsterdam, 1962), Vol. II.

[38] I. G. Kaplan, *Symmetry of Many-Electron Systems* (Academic Press, New York, 1975).

[39] M. Hamermesh, *Group Theory and Its Applications to Physical Problems* (Courier Corporation, 2012).

[40] M. A. Nielsen and I. L. Chuang, *Quantum Information and Quantum Computation* (Cambridge University Press, Cambridge, 2000).

[41] G. Fano and S. M. Blinder, in *Mathematical Physics in Theoretical Chemistry* (Elsevier, Amsterdam, 2019), pp. 377–400.

[42] E. Ovrum, Quantum computing and many-body physics, Master's thesis, University of Oslo, 2003.

[43] E. Ovrum, M. Hjorth-Jensen, Quantum computation algorithm for many-body studies, arXiv:0705.1928 v1.

[44] P.-O. Löwdin and O. Goscinski, The exchange phenomenon, the symmetric group, and the spin degeneracy problem, Int. J. Quantum Chem. **4**, 533 (1969).

[45] P. A. M. Dirac, *Quantum Mechanics*, 2nd ed. (Oxford University Press, London, 1935).

[46] H. F. Trotter, On the product of semi-groups of operators, Proc. Am. Math. Soc. **10**, 545 (1959).

[47] Héctor Abraham *et al.* (Qiskit Collaboration), *Qiskit: An Open-source Framework for Quantum Computing*, https://qiskit.org/ (2019).

[48] S. P. Jordan, Permutational quantum computing, Quantum Inf. Comput. **10**, 470 (2010).

[49] V. Havlicek, S. Strelchuk, and K. Temme, Classical algorithm for quantum SU(2) Schur sampling, Phys. Rev. A **99**, 062336 (2019).

[50] K. Choi, D. Lee, J. Bonitati, Z. Qian, and J. Watkins, Rodeo Algorithm for Quantum Computing, Phys. Rev. Lett. **127**, 040505 (2021).

[51] Z. Qian, J. Watkins, G. Given, J. Bonitati, K. Choi, and D. Lee, Demonstration of the Rodeo algorithm on a quantum computer, arXiv:2110.07747.

[52] E. A. Ruiz Guzman and D. Lacroix, Accessing ground state and excited states energies in many-body system after symmetry restoration using quantum computers, arXiv:2111.13080.